Detailed description of $K_L \to \pi^0 \nu\overline{\nu}$ Analysis

T. NAKAYA

V1.0

Contents

1 Introduction

This document provides supplemental description for the $K_L \to \pi^0\nu\overline{\nu}$ paper [1]. We describe the $K_L \to \pi^0\nu\overline{\nu}$ special run and the analysis in detail. The physics motivation for the decay $K_L \to \pi^0\nu\overline{\nu}$ is not discussed here, and it is mentioned in the paper [1] itself. The document will help the KTeV collaborators to understand the $K_L \to \pi^0\nu\overline{\nu}$ special run and the technical details of the analysis.

2 $K_L \to \pi^0\nu\overline{\nu}$ Special Run

During the 1996 KTeV data taking, we carried out a special run for the purpose of searching for the rare decay $K_L \to \pi^0\nu\overline{\nu}$ with $\pi^0 \to \gamma\gamma$ decay mode. The data were taken on December 21st and 22nd in 1996.

In the special run, we plugged 40 inch tungsten in the east beam to make one neutral hadron beam. The 40 inch tungsten was set between the Hyperon Magnet (NM2S2) and the Primary collimator. We put the MA in, but took the regenerator out. We also took TRD out, but did not put a He bug in the position of TRD. Therefore, the section of TRD was filled with air.

We took the runs listed in Table 1 with various conditions. The run 7639 was same condition as a standard E832 run without a regenerator beam. The runs 7643, 7644 and 7653 had the configuration with a smaller beam of which size was tuned by JAW collimator. The other runs were taken to collect more statistics with the high intensity setting (No Be absorber and a 8cm $\times$ 8cm beam). As a reference of the statistics, the number of $K_L \to 2\pi^0$ decays reconstructed in the Level-3 filter code is shown in Table 1. During the high intensity run, we found that there was no benefit of the high intensity due to the signal loss by accidental activities and due to more background events [2]. Therefore, we only used the run 7639 and 7653 for the analysis of $K_L \to \pi^0\nu\overline{\nu}$ search to achieve the best sensitivity. For the understanding of the background, the other runs would be also useful.

Run Number	Beam Size	Absorber	$\#K_L \to 2\pi^0$ decays in L3
7639	8cm $\times$ 8cm	20" Be IN	22,000
7643	4cm $\times$ 4cm	20" Be IN	2,200
7644	8cm $\times$ 2cm	20" Be IN	2,200
7645	8cm $\times$ 8cm	20" Be OUT	$> 3,000$
7647	8cm $\times$ 8cm	20" Be OUT	$> 50,000$
7648	8cm $\times$ 8cm	20" Be OUT	$\sim 5,000$
7649	8cm $\times$ 8cm	20" Be OUT	39,000
7651	8cm $\times$ 8cm	20" Be OUT	$\sim 11,000$
7652	8cm $\times$ 8cm	20" Be OUT	$\sim 9,000$
7653	4cm $\times$ 4cm	20" Be IN	$\sim 8,600$

Table 1: $K_L \to \pi^0\nu\overline{\nu}$ Special Run

In addition to the special run, we also collected $K_L \to \pi^0\nu\overline{\nu}$ triggers in the standard E832 runs. The beam trigger 15 in E832 is the $K_L \to \pi^0\nu\overline{\nu}$ trigger.

3 Trigger

3.1 Level-1 and Level-2 Trigger

The final observable particles in the decay $K_L \to \pi^0 \nu \overline{\nu}$ are two photons from a single π^0. In addition to the signal π^0, we do not have any other particles. Therefore, the Level-1 and Level-2 triggers are designed to accept exactly the two photons. In addition to two-photon events, the $K_L \to 2\pi^0$ decays were also collected for the purpose of normalization. The Level-1 trigger definition is:

$$
\begin{aligned}
&\mathrm{ET\_1BD} * \overline{\mathrm{V0} * \mathrm{V1}} * \overline{\mathrm{HA}} \\
&* \overline{\mathrm{RC6}} * \overline{\mathrm{RC7}} * \overline{\mathrm{RC9}} * \overline{\mathrm{RC10}} * \overline{\mathrm{SA2}} * \overline{\mathrm{SA4}} * \overline{\mathrm{CIA}} * \overline{\mathrm{CA}} * \overline{\mathrm{BA1} * \overline{\mathrm{BAHAD}}} \\
&* \mathrm{HCC\_24}.
\end{aligned}
$$

In the above description, the ET_1BD is the requirement that one of ET boards is fired. The turn-on threshold of the ET board is 3 GeV, and the efficiency of the ET board trigger is 80% at 4 GeV and nearly 100% at 6 GeV [3]. The HCC_24 is the HCC requirements with 2 or 4 clusters. The other trigger thresholds are set to be same as those used in E832. The BA gain was set to be low half during the high intensity run in which Be absorber was taken out.

3.2 Level-3 Trigger

In the Level-3 trigger, we require no reconstructed tracks in the events. We also reconstruct $K_L \to 2\pi^0$ decays as the same algorithm as the algorithm used in the E832 η_{00} trigger. For the two photon events, we reconstruct two hardware clusters. The z vertex is measured with an assumption that two photons come from a single π^0 decay, and the z vertex is required to be in the range between 100 and 162 m. The approximate expression of the z vertex is:

$$z = z_{CsI} - r_{12}/m_{\pi^0} \cdot \sqrt{E_1 \cdot E_2},$$

where z_{CsI} is the position of the calorimeter in the z axis, r_{12} is the distance between the two photons in the calorimeter, m_{π^0} is the π^0 mass and E_i is the energy of the i-th photon.

3.3 Trigger Rates

With the standard E832 beam size and with 20 inch Be absorber IN, the Level-1 trigger rate was around 20 kHz. The Level-2 trigger rate was around 3 kHz. In the Level-3 trigger, approximately 25% events were saved as either two photon candidates or $K_L \to 2\pi^0$ candidates.

3.4 Other Triggers

In addition to the $K_L \to \pi^0\nu\overline{\nu}$ triggers, we also collected the triggers listed in Table 2. The prescale factor for each trigger will be found in the run_summary file at the directory `~da_ktev/online_logs/run_summary` area on the ktev online computer.

4 Analysis

The analysis is carried out in two stages. The purpose of the first stage is to reduce the data size down to a handful number of events. By applying the veto requirements, we require the events to have exactly two photons and nothing else. You can skip to Section 4.2 if you want to see the specific selection criteria for the $K_L \to \pi^0\nu\overline{\nu}$ decay. The events passing the first stage are kept in the Ntuple file. At the second stage, the data analysis is performed with the Ntuple variables to search for the decay $K_L \to \pi^0\nu\overline{\nu}$ with the best achievable sensitivity.

Trigger No.	Purpose
Beam 2	Ke3 for CsI calibration (for E832)
Beam 6	E832 $K_L \to 3\pi^0$ trigger
Beam 8	90 degree accidentals
Beam 9	90 degree or muon accidentals
Beam 10	2V0 or 2V1 (for E832)
Beam 11	RC*SA3 for Photon Veto calibration
Beam 13	$K_L \to 3\pi^0$ trigger (same L1 trigger as $K_L \to \pi^0\nu\overline{\nu}$ trigger).
Beam 15	$K_L \to \pi^0\nu\overline{\nu}$ trigger
Calib 1	Laser
Calib 2	Laser Pedestal
Calib 3	Cosmic
Calib 4	DPMT Pedestal
Calib 5	???
Calib 10	FERA Pedestal

Table 2: Triggers in the $K_L \to \pi^0\nu\overline{\nu}$ special run

4.1 First Analysis Stage (Data Reduction)

In the first analysis stage, the standard KTeV analysis package (ktevana v4_05) is used. The analysis cuts are summarized in Table 3.

CUTs	Fraction of events
After the L3	100 %
NXUS=0, NYTR=0 AND NXTR=0	90 %
$\mathrm{ADC_{MA}} < 500$, $\mathrm{ADC_{RC}} < 2000$, $\mathrm{ADC_{SA}} < 500$ and $\mathrm{ADC_{HA}} < 300$	36 %
Four hardware cluster events	17 %
Events reconstructed as $K_L \to 2\pi^0$ decays	1 %
Two hardware cluster events	19 %
Two (hardware plus software) cluster events	10 %
Events with no fused cluster	9 %

Table 3: Summary of the first analysis stage.

The selection criteria applied in the first stage are:

1. A track is reconstructed, and the tracking variables NXUS, NYTR and NXTR are required to be exactly 0. About 10% of events have a track and are rejected.

2. Photon Veto ADC counts are reconstructed module by module. The maximum ADC count in each detector is selected, and is required to be less than 500 for MA, less than 2000 for RC, less than 500 for SA, less than 300 for HA. The thresholds of the cuts are pretty loose, and are tightened at the second stage. The calibration constants for the energy measurement of each detector are shown in Table 4. About 64% events have a hit in the photon veto detectors, and are rejected.

Detector	Energy/ADCcnt
MA, RC	1.65 MeV/cnt
SA, CIA	0.93 MeV/cnt
BA1	17.9 MeV/cnt
BA12	13.6 MeV/cnt
BA3	$\sim$ 35 MeV/cnt

Table 4: ADC count versus the energy for photon veto detectors

The maximum ADC distribution for each detector is shown in Figure 1.

3. For four-cluster events, we reconstruct $K_L \rightarrow 2\pi^0$ events. The mass of $2\pi^0$ is required to be between 470 and 550 MeV/c^2. The reconstructed z vertex is required to be between 100 and 160 m. The pairing χ^2 is required to be less than 50. Approximately 8% of four cluster events are reconstructed as the $K_L \rightarrow 2\pi^0$ events.

4. For two-cluster events, we reconstruct clusters again with the option of software clustering (IPACK=77 for KTCLUS). The distribution of the number of clusters is shown in Figure 2. In the figure, we clearly see events with more than two clusters. The number of clusters is required to be exactly two. In addition to the requirement, the events with a fused cluster (FUSEdCS=1) are rejected. The fraction of events whose have a fused cluster is only 4%.

4.2 Second Analysis Stage

The events passing the first stage are kept in a file with the following Ntuple variables listed in Table 5. The second stage analysis is carried out by using the variables in Table 5. If you want to look into the data, you can

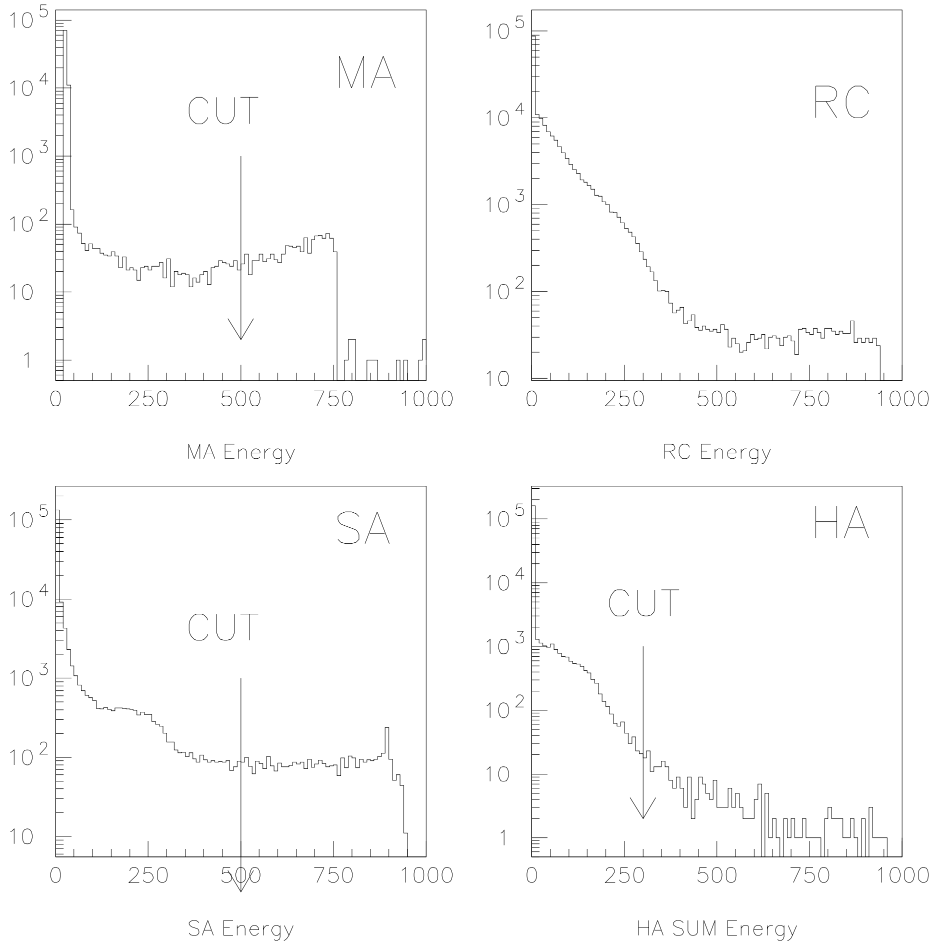

Figure 1: The distribution of the maximum ADC count for MA, RC, SA and HA. The point of the cut is shown by an arrow. The overflow events are not shown in the above histograms.

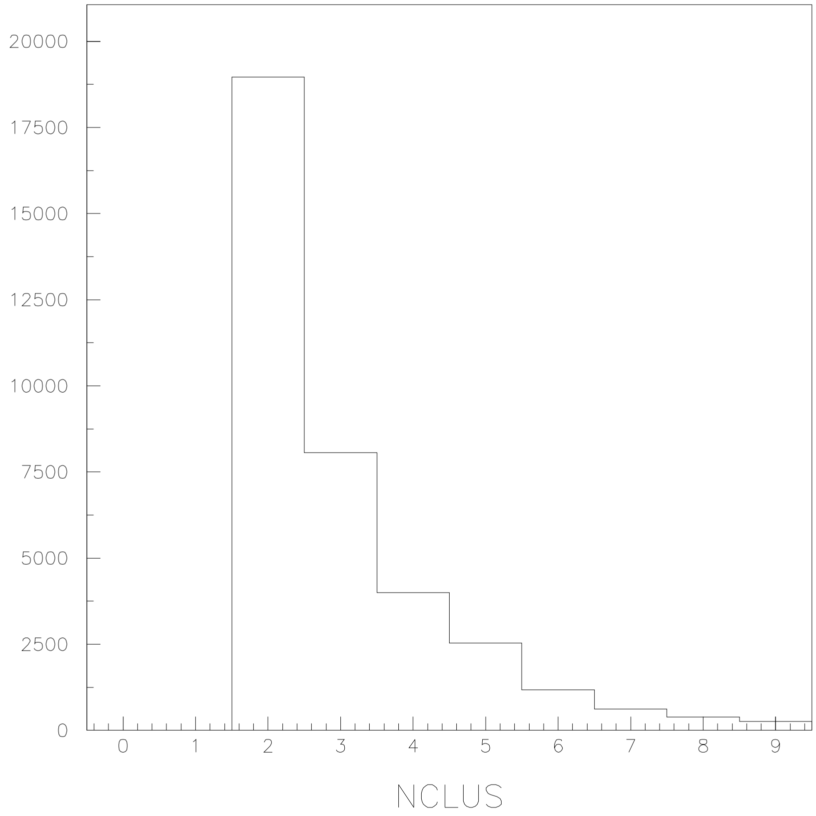

Figure 2: The number of software plus hardware clusters for the events in which two hardware clusters are reconstructed. The events with more than two clusters are background events from $K_L \to 3\pi^0$, $K_L \to 2\pi^0$ and neutron interactions.

Variables	Comments
ievt	Event Number
irun	Run Number
pt	The two photon P_T with a π^0 mass assumption. (0 for $K_L \to 2\pi^0$).
zvtx	Z vertex
et	Total Energy (Energy sum of the clusters)
px, py	The x and y components of the P_T
ecls(4)	The energy of cluster. (ecls(1) > ecls(2) > ecls(3) > ecls(4)).
xcls(4), ycls(4)	The x and y position of clusters
xecen, yecen	The x and y center of energy for $K_L \to 2\pi^0$ events
mk2pi0	Two π^0 mass (0 for $K_L \to \pi^0\nu\overline{\nu}$ events).
ema	The maximum ADC counts in MA.
erc	The maximum ADC counts in RC.
esa	The maximum ADC counts in SA.
eha	The maximum ADC counts in HA.
eca	The maximum ADC counts in CA.
eba1l,2l,3l	The maximum ADC counts in left-side BA1,2,3
eba1r,2r,3r	The maximum ADC counts in right-side BA1,2,3
ndch1,2,3,4	The sum of the hits in the Drift chamber 1,2,3 and 4.

Table 5: Ntuple variables for the $K_L \to \pi^0\nu\overline{\nu}$ Analysis

use the ntuple files `~nakaya/kpinn/his/kpinn_new.his` for the run 7653, and `~nakaya/kpinn/his/kpinn_7643.his` for the run 7643 on ksera.

4.2.1 Selection Criteria for $K_L \to \pi^0\nu\overline{\nu}$

For the two-photon events, the z vertex of the decay $\pi^0 \to \gamma\gamma$ is calculated with the same expression in the Level-3 trigger (see Section 3.2). With the z decay position, we calculate the transverse momentum, P_T, of the π^0 from the beam center. The expression of P_T is:

$$P_T = (E_1 + E_2) \times r_{\text{(from beam center)}}/(z_{CsI} - z),$$

where $r_{\text{(from beam center)}}$ is the distance between the center of energy of two photons and the beam center. In the analysis, the beam center is chosen as the beam center of the standard E832 beam (x=0.15 m, y = 0.0m). We did not use the real beam center of the narrower beam (x=0.13m, y = 0.0m). The original motivation to select the E832 beam center is to avoid the background events located at the tail of the beam halo at the side of JAW collimators (see Figure 12). At the end of the analysis, we find that the selection of either beam center does not affect the final result.

The selection criteria in the analysis are summarized in Table 6. The principle of the search is to select the events likely $K_L \to \pi^0\nu\overline{\nu}$ decay, which have a high P_T π^0 with nothing else. As a reference, the numbers of expected background events in the Monte Carlo (MC) simulation are also shown in the table. If you have no knowledge of the background events, please glance Section 6 or read the paper [1] at first. After applying all the cuts mentioned in Table 6, We have one $K_L \to \pi^0\nu\overline{\nu}$ candidate event which is concluded to be a background in Section 6.

The number of events at each stage roughly looks consistent between data and the MC sum. At some stages, you may see an inconsistency between data and the MC sum. The inconsistency could be due to the background from neutron interaction and the background from Λ scattered in the collimator.

CUT	# events	A($\pi^0\nu\overline{\nu}$)	N($2\pi^0$)	N($3\pi^0$)	N(Λ)	N(Ξ^0)
After 1st stage	125,016	27.0 %	609	4,876	88,351	9,225
125 < z < 157 m	49,067	22.0 %	392	3,045	37,248	4,693
$160 < P_T < 260$ MeV/c	1,677	11.5 %	9	68	88	228
Tight Photon Veto cut	177	8.5 %	1.1	11	15	13
Chamber cuts	128	7.6 %	1.1	9.5	13	12
$E_T < 35$ GeV	30	5.2 %	0.18	9.4	0.15	1.1
$P_X/P_T > -0.8$	3	3.9 %	0.18	0	0.15	0.6
$\frac{E_{\gamma 1}-E_{\gamma 2}}{E_{\gamma 1}+E_{\gamma 2}} < 6$	1	3.6 %	0.18	0	0.15	0.3

Table 6: Summary of the second analysis stage. "# events" is the number of events for the data after applying the cut, A($\pi^0\nu\overline{\nu}$) is the acceptance for the decay $K_L \to \pi^0\nu\overline{\nu}$, N($2\pi^0$) is the number of expected background events from $K_L \to 2\pi^0$ decay, N($3\pi^0$) is the number of expected background events from $K_L \to 3\pi^0$ decay, N(Λ) is the number of expected background events from $\Lambda \to n\pi^0$ decay, and N(Ξ^0) is the number of expected background events from $\Xi^0 \to \Lambda\pi^0$ decay. The $K_L \to \gamma\gamma$ background is not shown here since the events are completely eliminated with the P_T cut. The ratio of the data statistics to the MC statistics was 0.18 for any kaon decays, 0.83 and 0.15 for Λ decay before and after applying the BA cut (in Tight Photon Veto cut), 0.56 and 0.1 for Ξ^0 decay before and after applying the BA cut. For example, if we have one remaining event in the $K_L \to 2\pi^0$ decay in the MC, the expected background level was calculated to be $1 \times 0.18 = 0.18$ events.

In addition, the poor simulation in the upstream region of the detector (< 100 m) could cause the inconsistency, too.

The details of the selection criteria are:

1. In order to veto background events from neutron interactions in the MA and the vacuum window, the z vertex is required to be between 125 and 157 m. This cut effectively eliminates the events from neutron interactions where a single π^0 is produced. The z vertex resolution is expected to be approximately 30 cm. The z distributions for data and $K_L \to \pi^0 \nu \overline{\nu}$ MC are shown in Figure 3. The fraction of events from neutron interactions in the vacuum window and the fraction of $\Lambda \to n\pi^0$ events are roughly figured out in the data (also see Figure 4).

2. To eliminate the $K_L \to \gamma\gamma$ decays which have a zero P_T and to suppress the $\Lambda \to n\pi^0$ events which have a P_T as high as 104 MeV/c, we selected the events with the P_T between 160 and 260 MeV/c. The P_T distribution is shown in Figure 4. Before applying this cut, the events are dominated by $\Lambda \to n\pi^0$ decay.

3. In order to select events with exactly two photons, the cut on the photon veto detectors were applied for ema < 40, erc < 50, esa < 1, eha < 50, eba1l < 25, eba2l < 25, eba3l < 12, eba1r < 20, eba2r < 20, eba3r < 10. With Table 4, the above photon veto thresholds can be reconstructed with an energy unit. Remind that the above cuts are imposed over the offset of the ADC readout threshold. The typical ADC readout threshold is around 5 ADC counts. For example, the SA energy threshold is $(1 + 5) \times 0.93 \sim 5$ MeV. With the above cuts, the signal loss due to accidental activities is $< 1\%$ for the MA, $< 1\%$ for the RC, 10% for the SA, $< 1\%$ for HA, 1% for BA Right, and 18% for BA Left. Note that the beam hit the left side of BA. Therefore, the right side of BA was very quiet. The tight SA requirement is crucial to catch

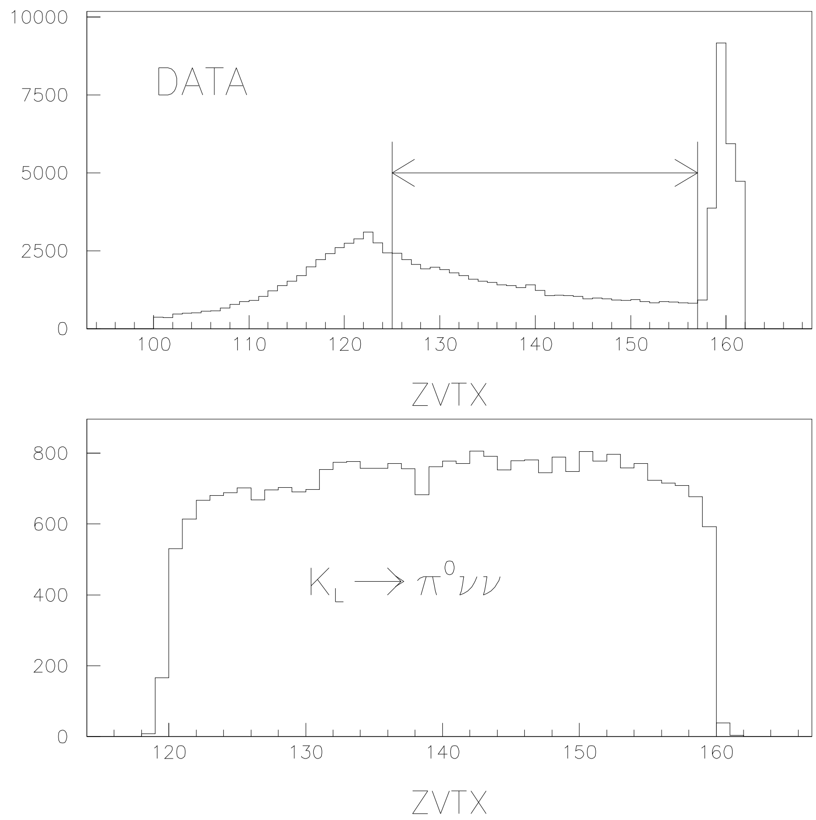

Figure 3: The z vertex distribution for data and $K_L \to \pi^0 \nu \overline{\nu}$ MC events

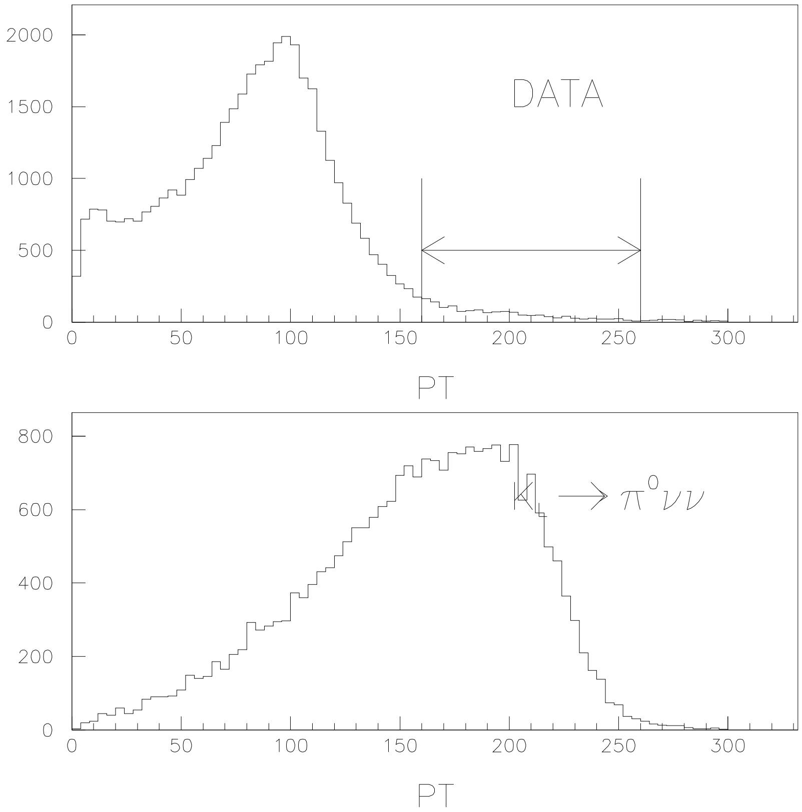

Figure 4: The P_T dsitribution for data and $K_L \to \pi^0\nu\overline{\nu}$ MC events. The events are dominated by $\Lambda \to n\pi^0$ decay which have a Yacobian peak at $P_T = 104$ MeV/c.

a low energy particle from neutron interactions in the detector (at the Drift Chambers and at the He bugs). The tight BA requirements are also crucial to detect a neutron. The 18% signal losses by accidental activities in the BA Left consists of 4% in the BA1, 14% in the BA2 and 11% in the BA3. The largest signal loss by the BA2 is due to the lowest energy threshold which we did not know when we determined the threshold. At the end of the analysis, it is found that the BA2 cut is insensitive to the background rejection. Figure 5 shows the maximum ADC distribution for SA and BA3-left which cause the large signal loss by accidental activities.

4. In order to veto a charged particle which comes from the decay in flight or from neutron interactions, we impose cuts on the number of hits in the Drift Chambers. The number of hits is required to be less than 16 for DC2, and less than 4 for DC3 and DC4. The signal loss by accidental activities is $< 1\%$ for DC2, 3% for DC3 and 10% for DC4. The number of hits required above is determined to find and to reject one track in a downstream chamber (DC3 or DC4), which should have 4 hits. The hit requirement on DC2 was found to be insensitive for the background rejection. The hit distributions of DC3 and DC4 are shown in Figure 6. In the DC4 hit distribution, you can find the peak at 4 hits, which is a result that a charged particle passes through 4 planes (x, x', y and y' planes) of the chamber.

5. The total energy deposit in the CsI, which is the sum of the two cluster energy, is required to be less than 35 GeV to suppress the background events from $\Lambda \to n\pi^0$ and $\Xi^0 \to \Lambda\pi^0$ decays. The total energy distribution is shown in Figure 7 for data, $K_L \to \pi^0\nu\overline{\nu}$, $\Lambda \to n\pi^0$, and $\Xi^0 \to \Lambda\pi^0$ MC events. Originally, the 35 GeV cut was chosen to suppress the $\Lambda \to n\pi^0$ and $\Xi^0 \to \Lambda\pi^0$ events to be less than 0.1 expected events in the signal region. However, at the end of the analysis, the expectation is grown up to 0.18 $\Lambda \to n\pi^0$ events and 0.3 $\Xi^0 \to \Lambda\pi^0$

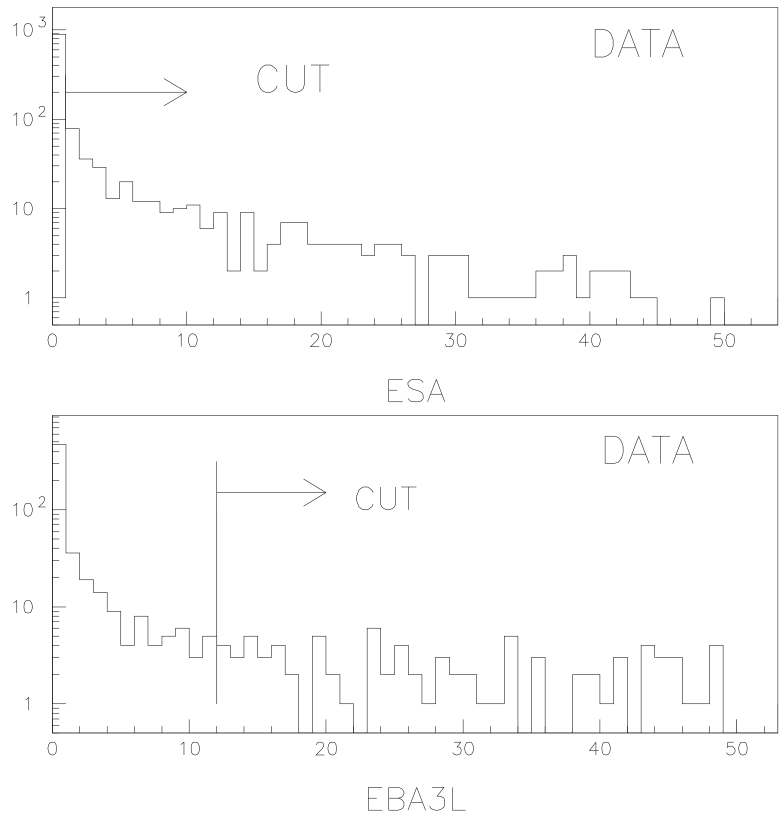

Figure 5: The maximum ADC distribution for the SA (top plot) and the BA3-left (bottom plot).

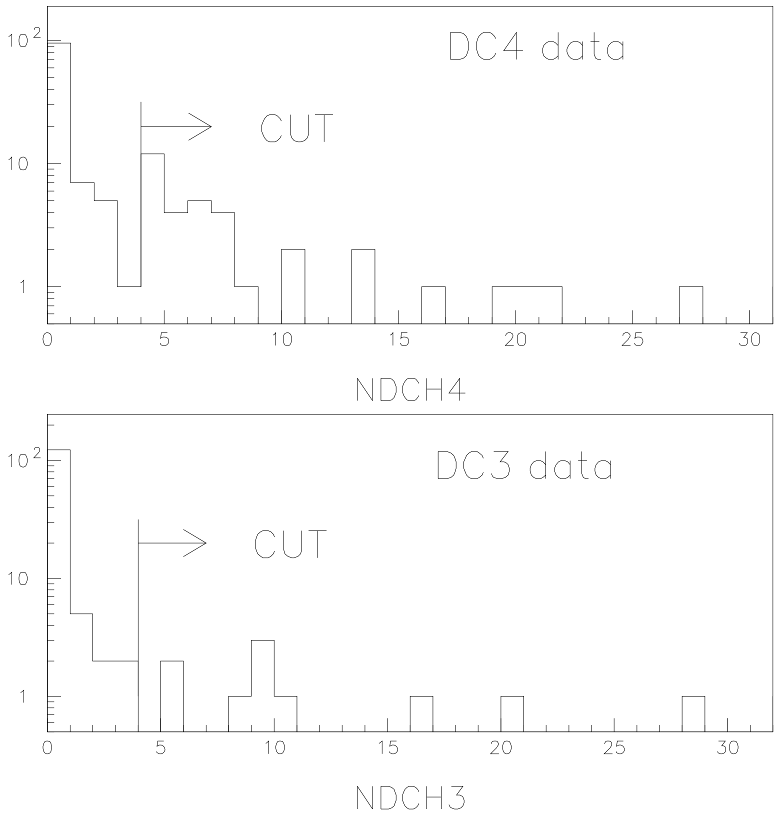

Figure 6: The hit distribution for DC4(top plot) and DC3(bottom plot).

events due to the improvement (update) of ktevmc simulation. This cut is also effective to suppress $\Lambda \to n\pi^0$ events where the Λ is scattered in a collimator.

6. The fraction of the horizontal transverse momentum to the total transverse momentum, P_x/P_T, is required to be greater than -0.8 to suppress the $K_L \to 3\pi^0$ background events which decay upstream of the MA. The topology of the background is drawn in Figure 8. Photons from different π^0s can pass through the two holes of MA while the remaining photons go undetected. The decay vertex position of events which are mis-reconstructed as a single π^0 can be shifted downstream into the fiducial region. These events can be identified by their large horizontal transverse momentum, P_x. The P_x/P_T distributions are shown in Figure 9 for data and the $K_L \to 3\pi^0$ background MC events.

7. We impose the cut on the ratio of the maximum photon energy to the minimum photon energy. The ratio is required to be less than 6. The discussion of this cut is a little bit long here. If you are not interested in this specific cut, you can skip the next section.

   The motivation of this cut is to reject events in which one cluster had significantly higher energy than other cluster had. For the $K_L \to \pi^0\nu\overline{\nu}$ decay, about 90% of the events pass this cut as shown in Figure 10 since the two photons from a single π^0 tends to have symmetric energy. Originally, the cut was found to be effective and was applied in the E832 2γ trigger [4] when we looked for the $K_L \to \pi^0\nu\overline{\nu}$ decay. The source of the background is unclear even now. Three kinds of background sources are guessed: (1) one higher energy photon from $\Lambda \to n\pi^0$ decay and an another accidental low-energy photon, (2) one photon from $\Lambda \to n\pi^0$ decay and the neutron hitting CsI as a fake photon, (3) one photon from the mother Ξ^0 decay and other photon from daughter Λ decay.

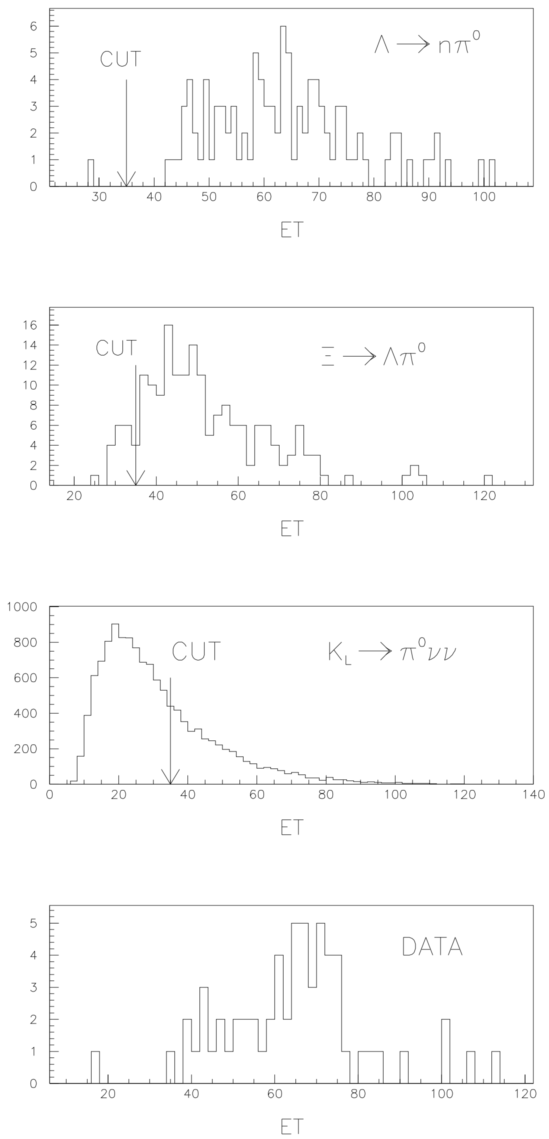

Figure 7: The E_T distribution for $\Xi^0 \to \Lambda\pi^0$, $\Lambda \to n\pi^0$ and $K_L \to \pi^0\nu\overline{\nu}$ MC events with $160 < P_T < 260$ MeV/c and $125 <$ zvtx < 157 m. The data is shown with all the cuts mentioned in the paper except for the E_T cut.

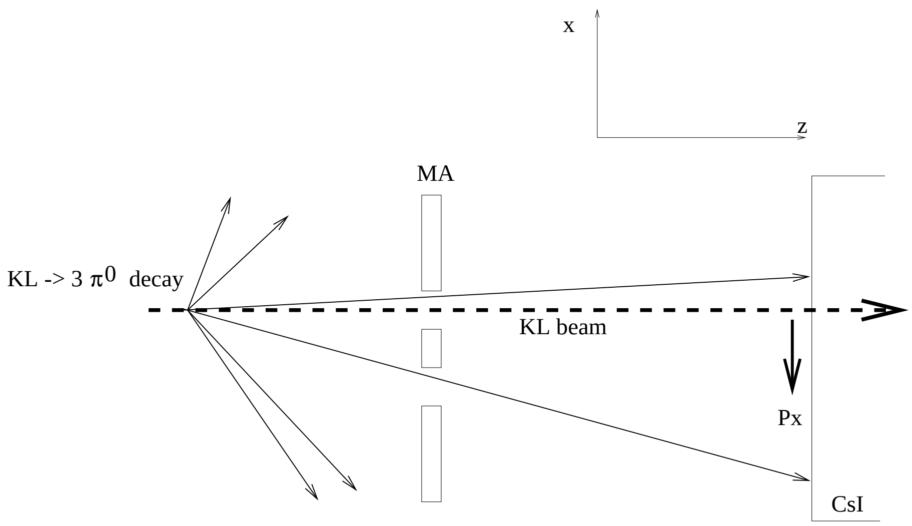

Figure 8: The topology of the $K_L \to 3\pi^0$ background where two photons pass through two MA beam holes. As the result, this background event have a large horizontal transverse momentum.

The first and the third background were not proved in the MC, but the MC could not be perfect. We never check the possibility of the second background.

Even if the background source is unclear, we know that the events removed by the cut are not likely $K_L \to \pi^0 \nu \overline{\nu}$ events. For the $K_L \to \pi^0 \nu \overline{\nu}$ MC events passing the cuts mentioned before, the mean energy of the higher energy photon is 15.6 GeV, the mean of the lower energy photon is 6.5 GeV, and the mean of the two-photon energy ratio is about 2.4. For the $\Xi^0 \to \Lambda \pi^0$ MC events, the mean of the two-photon energy ratio is about 3.2 where the mean of the higher energy photon is 23.7GeV and the mean of the lower was 7.4 GeV. The $\Xi^0 \to \Lambda \pi^0$ decay has the higher mean of of the two-photon energy ratio mainly due to the higher momentum of the π^0 and the energy threshold of the clustering. The energy threshold of the clustering is around $2 \sim 3$ GeV. The higher

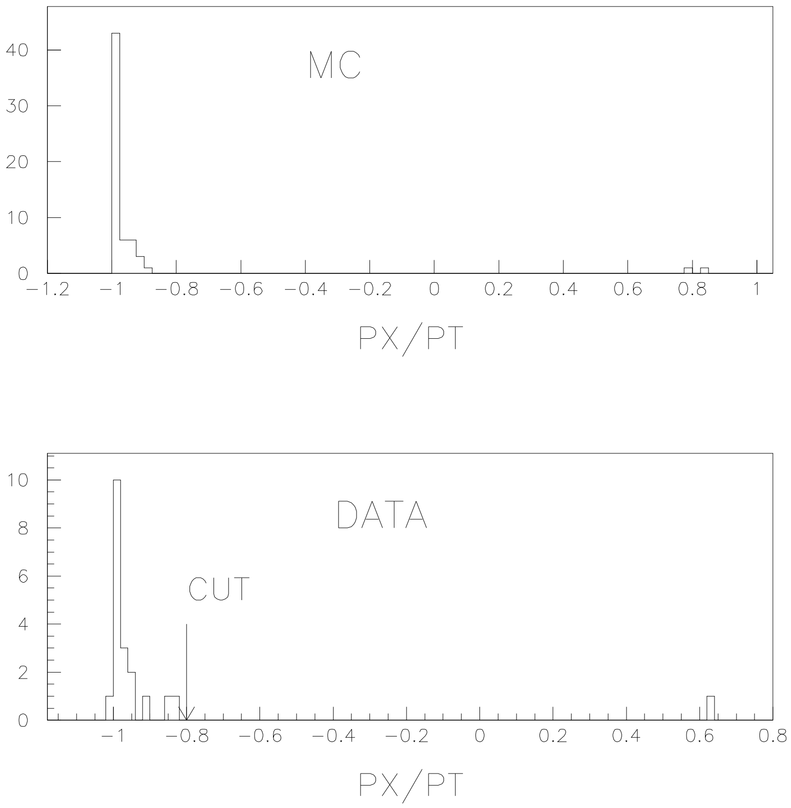

Figure 9: The P_x/P_T distribution for $K_L \to 3\pi^0$ MC events and data.

energy π^0 from the $\Xi^0 \to \Lambda\pi^0$ decay has larger phase space in the two-photon energy ratio. The cut on the two-photon energy ratio prefers to save the decay $K_L \to \pi^0\nu\overline{\nu}$ that the $\Xi^0 \to \Lambda\pi^0$. However, the observed distribution on the two photon energy asymmetry is not explained in the MC. In the MC simulation, the background level before applying this cut is small (the Ξ^0 decay background level is estimated to be 0.6 without this cut). We know that this unknown background exists when we looked into E832 data (Trigger 15) prior to this analysis [4]. Though we do not fully understand all kinds of background sources in the two photon data, we apply this cut in the analysis in order to distinguish the signal from the background as much as possible.

Note that this cut is very similar as the cut that we set the upper energy limit (20 GeV or so) for each photon. In the case, the cut definitely favors to reject Λ and Ξ^0 events.

As a reference, the two-photon energy ratio distribution is shown in Figure 10 for data, $\Xi^0 \to \Lambda\pi^0$ and $K_L \to \pi^0\nu\overline{\nu}$ MC events. The events with high asymmetry photons in $\Xi^0 \to \Lambda\pi^0$ may be due to just low MC statistic since two photons in the events come from the secondary $\Lambda \to n\pi^0$ decay.

4.2.2 Selection Criteria for $K_L \to 2\pi^0$

For $K_L \to 2\pi^0$ sample, we apply exactly same photon veto cuts and chamber cuts as for the $K_L \to \pi^0\nu\overline{\nu}$. In addition to the cuts, the following cuts are applied to select $K_L \to 2\pi^0$ events.

1. The 2 π^0 mass is between 475 and 520 MeV/c^2.
2. The z vertex is between 125 and 157 m.
3. The center of energy in the x axis is between 0.09 and 0.21 m, and the center of energy in the y axis is between -0.06 and 0.06 m.

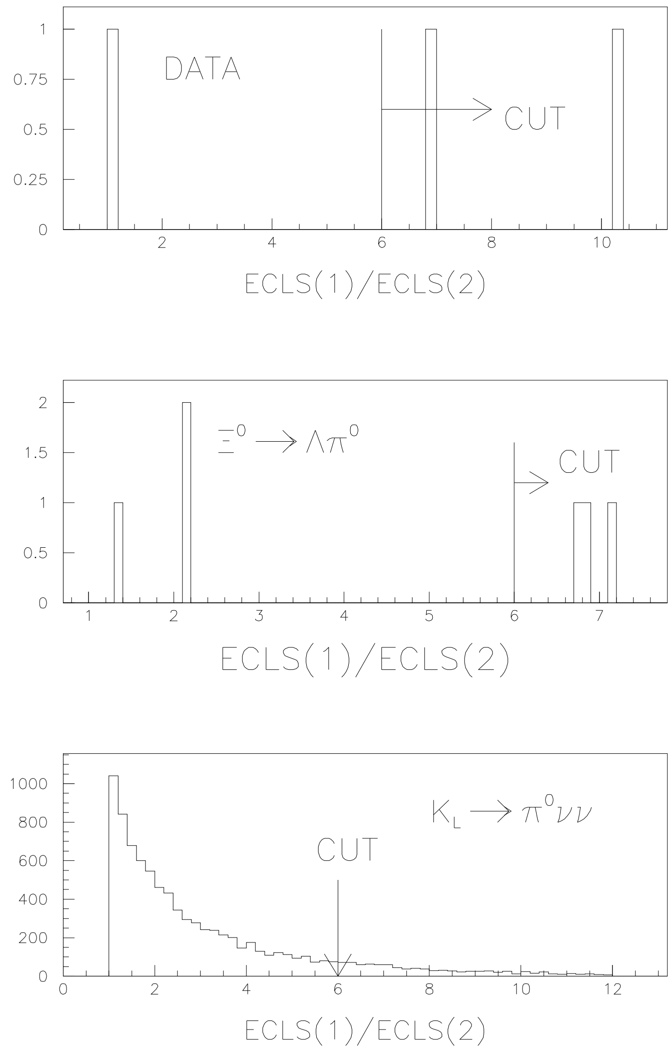

Figure 10: The ratio of the maximum photon energy to the minimum photon energy for data, $\Xi^0 \to \Lambda\pi^0$ MC and $K_L \to \pi^0\nu\overline{\nu}$ MC with all the cuts except for this cut.

4. The total energy is less than 220 GeV.

The $2\pi^0$ mass distribution for the final $K_L \to 2\pi^0$ events is shown in Figure 11. After all the cuts, we have 4326 $K_L \to 2\pi^0$ events with an estimated

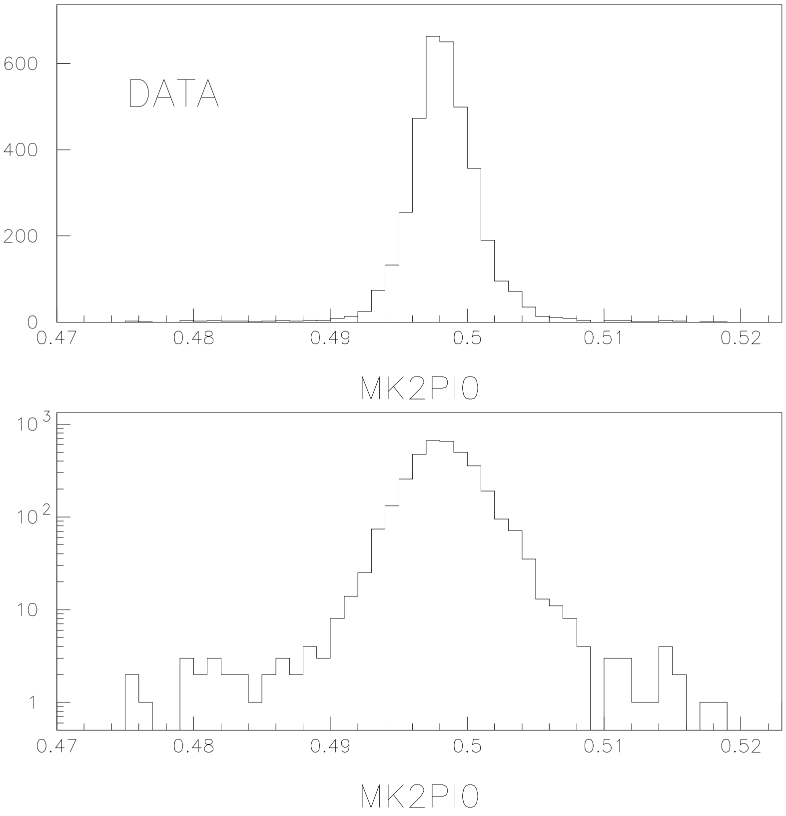

Figure 11: The 2 π^0 mass distribution for $K_L \to 2\pi^0$ events. The background level estimated from the mass side-bands was about 1 %. The top plot is shown in linear scale and the bottom plot is shown in log scale.

background of 44 events from the mass side-bands. The summary of the events selection for the $K_L \to 2\pi^0$ decay is shown in Table 7.

CUT	N($K_L \to 2\pi^0$)	A($K_L \to 2\pi^0$)
$475 < M_{2\pi^0} < 520\ MeV/c^2$	12,500	12.5 %
125 < z < 157 m	9,389	10.3 %
$0.09 < x_{CE} < 0.21$, $\lvert y_{CE} \rvert < 0.06$ m	9,032	10.3 %
$E_T < 220$ GeV	9,026	10.3
Tight Photon Veto cut	4,995	7.5 %
Chamber cuts	4,326	6.8 %

Table 7: Summary of the $K_L \to 2\pi^0$ event selection. N($K_L \to 2\pi^0$) is the number of $K_L \to 2\pi^0$ candidate events without subtracting background events. A($K_L \to 2\pi^0$) is the acceptance for the $K_L \to 2\pi^0$ decay, which is discussed in Section 5. $x(y)_{CE}$ is the center of energy in the x(y) axis in the CsI. Note that N($K_L \to 2\pi^0$) includes the background events from the $K_L \to 3\pi^0$ decay which are removed significantly by the tight photon veto cut.

5 Simulation, Acceptance and the Single Event Sensitivity

The $K_L \to \pi^0 \nu \overline{\nu}$ special run is simulated with the standard KTeV/E832 Monte Carlo (MC) simulation (ktevmc) V4_05 with the following modification.

1. The JAW collimator is installed to simulate the smaller hadron beam.

2. The Regenerator is removed.

3. The E_T board trigger is simulated.

The cradle file for this MC is `~nakaya/kpinn/mc/v4_05/mckpinn.cra` on ksera machine.

The narrow beam provided by the JAW collimator is checked for $K_L \to 2\pi^0$ events between data and MC. They are good agreement as shown in Figure 12.

With the MC, we calculate the acceptance for the $K_L \to \pi^0 \nu \overline{\nu}$ and $K_L \to 2\pi^0$ decays. We generate events in the z range between 120 and 160 m, and in the momentum range between 20 and 220 GeV/c. The acceptance is calculated to be 3.6% for the decay $K_L \to \pi^0 \nu \overline{\nu}$, and 6.8 % for the decay $K_L \to 2\pi^0$. With the numbers, the single event sensitivity in this experiment is:

$$
\begin{aligned}
SES(K_L \to \pi^0 \nu \overline{\nu}) &= BR(K_L \to 2\pi^0)/N(K_L \to 2\pi^0) \times \frac{A(K_L \to 2\pi^0)}{A(K_L \to \pi^0 \nu \overline{\nu})} \\
&= (9.36 \pm 0.2) \times 10^{-4}/(4326 - 44) \times \frac{6.75}{3.69} \\
&= [4.00 \pm 0.06(stat.)] \times 10^{-7},
\end{aligned}
$$

where $N(K_L \to 2\pi^0)$ is the number of $K_L \to 2\pi^0$ events, and $A(K_L \to X)$ is the acceptance of the decay $K_L \to X$.

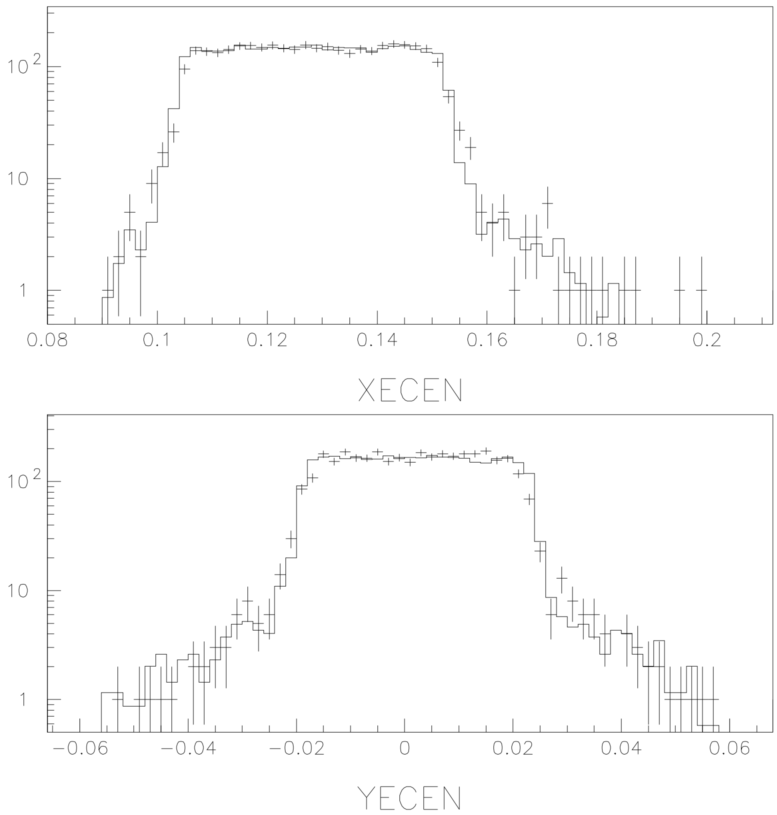

Figure 12: The x and y beam shape (the center of energy) at the CsI for $K_L \rightarrow 2\pi^0$ decay for data and MC . The cross dot shows data, and the histogram shows MC. They are in good agreement in both views.

.

6 Background Estimation

In Section 4, we observe one event in the signal region. In the paper [1], we conclude that the event is background. We explain the background estimation in detail in this section.

6.1 Background from Kaon decays

The number of background events from kaon decays is estimated based on the KTeVMC simulation. The $K_L \to 2\pi^0$, $K_L \to 3\pi^0$, $K_L \to \gamma\gamma$, $K_L \to \pi^0\gamma\gamma$, *kcpipipi* and K_{e3} decays are simulated. The kaon decays for background study are generated in the z range between 80 and 180 m, and in the momentum range between 10 and 510 GeV/c. We simulated 5.5 times more statistics than data, which corresponds to 7×10^{-8} single event sensitivity (SES) for the signal. The events in the MC are normalized with observed $K_L \to 2\pi^0$ events. In the level of 6×10^{-8} S.E.S, we have one background event from the decay $K_L \to 2\pi^0$ in the MC. The estimated number of background is calculated to be 0.18 events. In the paper [1] and this document, we do not mention the $K_L \to \pi^0\gamma\gamma$, $K_L \to \pi^+\pi^-\pi^0$ and K_{e3} decays which are eliminated at the early stage in the analysis.

A reader wonders that the background level from the kaon decays (such as $K_L \to 3\pi^0$ decay) depends on the response of the photon veto at the low energy ($\sim$ 10 MeV). We also relaxed the veto threshold up to 100 MeV for the events in the MC, and we do not have any additional events appeared.

6.2 Background from Λ and Ξ^0 decays

The estimated number of the background events from the Λ and Ξ^0 decays is included in the number given by the neutron interaction background in Section 6.3 because a neutron exists in the Λ and Ξ^0 decays. Though the background events with a neutron is estimated based on data, it is important to estimate the background events from Λ and Ξ^0 decays independently in the MC to compare the data with the MC in the low P_T region.

The *lnpi* decay and the *caslp* decay with the *lnpi* and *lppi* decays are simulated. The Λ rare decays listed in the PDG [5] are also simulated and are found to be negligible. The Λ decays are generated in the z range between 90 and 180 m, and in the momentum range between 40 and 500 GeV/c, and the Ξ^0 decays are generated in the z range between 40 and 187 m, and in the momentum range between 40 and 500 GeV/c. The Ξ^0 decays are generated from the far upstream because the Ξ^0 decay produces the secondary Λ which can have a higher P_T than the primary one. The relative flux between Λ and Ξ^0 is preliminary measured to be 100 : 7 at the $z = 90$ m in E799 [6]. In addition, there is a prediction of the relative flux to be 100 : 4.2 at the $z = 90$ m [7]. In this analysis, the 100 : 7 relative flux for Λ and Ξ^0 is used because it well reproduces the P_T spectrum of the data. Please note that the final background estimation does not depend on the value of the flux since we estimate the background events from data.

The absolute flux is normalized in the final P_T distribution in Figure 3 in the paper [1]. For events in the MC, the neutron veto by the BA is not applied. We use the veto inefficiency measured in the $\Lambda \to n\pi^0$ sample when we calculate the flux in the absolute normalization.

Taking care of the neutron detection inefficiency mentioned in Section 6.3.1, we simulated about 7 times more $\Lambda \to n\pi^0$ decays and 10 times more $\Xi^0 \to \Lambda\pi^0$ decays than data, which corresponds to 6×10^{-8} SES and 4×10^{-8} SES, respectively. In the signal region, we had one $\Lambda \to n\pi^0$ event and three $\Xi^0 \to \Lambda\pi^0$ events. Therefore, the number of background is estimated to be $1/7 + 3/10 = 0.44$ events from the Λ and Ξ^0 decays.

6.3 Background from Neutron Interactions

In the paper [1], we conclude that the final remaining event is from neutron interactions. Neutrons which interact with material such as the vacuum window and drift chambers can produce one or more π^0s. An interactions which produces multiple π^0s is a potential background source since the z vertex can be misreconstructed inside the fiducial volume when only two of the photons are detected. The neutron which remains in the final state can be used to suppress this background.

In addition to this multiple π^0 production, the η production in neutron interactions is also the background source. In 1996 KTeV winter data in the two-photon trigger, we find about 400 $\eta \to \gamma\gamma$ events in the vacuum window [8]. In the same trigger, we have about $60,000$ $K_L \to \gamma\gamma$ events. The relative ratio between $K_L \to \gamma\gamma$ and $\eta \to \gamma\gamma$ is calculated to be $60000 \div 40 = 150$. With $BR(K_L \to \gamma\gamma) = 6 \times 10^{-4}$, the rate of $\eta \to \gamma\gamma$ at the vacuum window corresponds to 4×10^{-6} in the unit of the kaon branching ratio. Considering ten times more material in the KTeV spectrometer than that of the vacuum window, the above $\eta \to \gamma\gamma$ rate is estimated to be around 4×10^{-5}. This rate looks pretty high than the $SES(K_L \to \pi^0\nu\overline{\nu})$. Note that the above $\eta \to \gamma\gamma$ rate depends on the veto threshold. We use very tight thresholds in this analysis compared with the standard E832 analysis. Therefore, the $\eta \to \gamma\gamma$ rate should be suppressed than the above expectation ($\sim 4 \times 10^{-5}$), though we do not have a concrete number. The $\eta \to \gamma\gamma$ background has also a neutron in the final state, and is included in the following estimation.

The most strong evidence to support the last remaining event as background from neutron interactions is the existence of the additional events far beyond the kinematical limit of both K_L and Λ decays in the P_T distribution.

To estimate the background level, we studied the BA efficiency with $\Lambda \to n\pi^0$ sample at first.

6.3.1 BA efficiency for a neutron

The BA efficiency for a neutron is studied by using the sample of the $\Lambda \to n\pi^0$ decay. The $\Lambda \to n\pi^0$ events are collected with the following selection criteria.

1. We impose exactly same photon veto cuts used for $K_L \to \pi^0 \nu \overline{\nu}$ search except for the BA cuts.

2. The z vertex is required to be between 125 and 135 m (upstream), which prefers to the decay $\Lambda \to n\pi^0$.

3. The P_T is required to be less than 150 MeV/c to suppress the neutron background in the MA.

With the above cuts, the PT distribution for data is shown in Figrue 13. In the figure, we also show the P_T distribution with the requirements of hits in BA1, BA2 and BA3. By counting the number of events in the P_T region between 75 and 150 MeV/c, we measure the efficiency of the BA for a neutron (see Table 8). With the result in Table 8, we conclude that the BA

BA Section	Efficiency % (Number of events)
No Requirement	100 % (9020)
BA1 ON	44 % (3945)
BA2 ON	70 % (6302)
BA3 ON	80 % (7204)
ALL BA OFF	18 % (1603)

Table 8: BA Efficiency for a neutron in $\Lambda \to n\pi^0$ sample

efficiency for a neutron is 82%$(= 1 - 0.18)$. The above BA efficiency includes the volunteer of accidental activities. Without the accidental activities, the true BA efficiency for a neutron is a couple of percentage less than the above number. For example, define "x" as the true BA efficiency for a neutron, and "y" as the accidental activity. The components of 82% are: (1) a neutron firing BA, (2) an accidental firing the BA, (3) Coincidence of a neutron and an accidental firing BA. Therefore, the 82%(0.82) is expressed as:

$$0.82 \quad = \quad x + y - x * y,$$

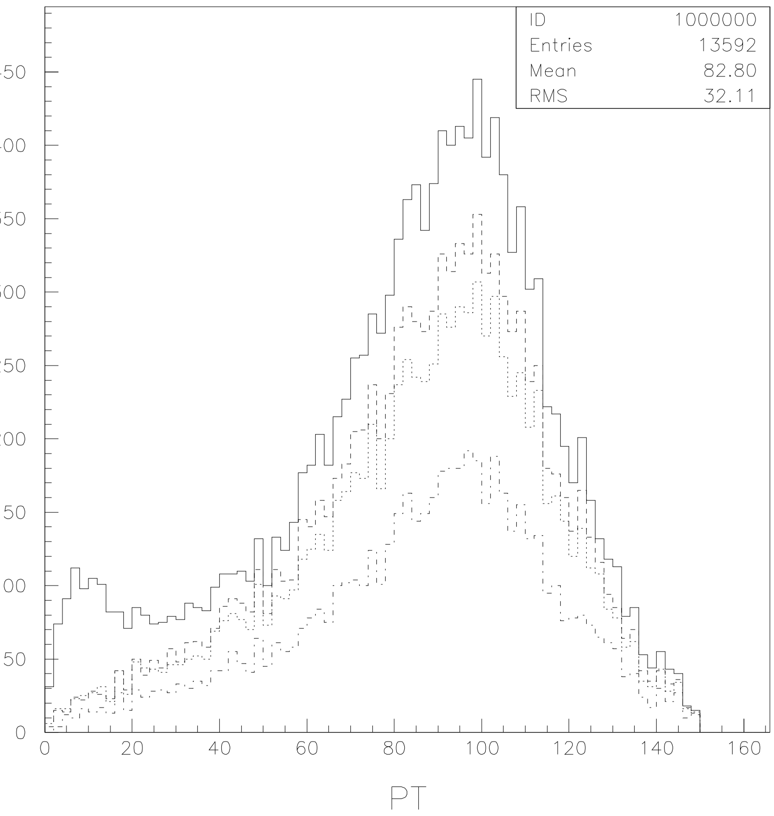

Figure 13: The P_T distribution for $\Lambda \to n\pi^0$ events. The dashed line shows the P_T with hits on BA3, the dotted line with hits on BA2 and the dash-dotted line with hits on BA1. The BA thresholds are same as those defined in the $K_L \to \pi^0 \nu \overline{\nu}$ analysis.

where x is the component (1), y is the component (2) and the $x * y$ is the component (3). We measure the "y" in the accidental data and the value is 0.17. Therefore,

$$\begin{aligned} 0.82 &= x + 0.17 - 0.17x \\ x &= 0.78 \end{aligned}$$

As a result, the true BA efficiency for a neutron is 78%. Since we use the same data to study the BA efficiency, we use the 82% for the $K_L \to \pi^0 \nu\overline{\nu}$ analysis due to the same level of accidental activities.

6.3.2 The neutron interaction background

The background level from neutron interactions is estimated with the study of the fraction of the activities in BA. Note that this background estimation includes the background from $\Lambda \to n\pi^0$ and $\Xi^0 \to \Lambda\pi^0$ decays which result in a neutron in the final state.

At first, we take the BA veto out, which results in 37 events in the $K_L \to \pi^0 \nu\overline{\nu}$ signal box. Those events are classified into three categories:
(1) The events which has only a neutron hitting the BA,
(2) The events which has both a neutron and a photon hitting the BA.
(3) The events which has no neutron nor no photon hitting the BA.
The category (1) includes the background events from $\Lambda \to n\pi^0$ decay. In addition, the η production in the detector also belongs to this category. The multiple π^0 production in the neutron interaction in which a photon does not go down to BA is also in this category. The category (2) is most likely events from neutron interaction where multiple π^0's are produced and at least one photon goes down to BA. The category (3) includes a kaon decay. We found that the contribution from kaon decays is negligible in the MC (~ 1.4 events). We define the fraction of the events in the above three categories as f_1, f_2 and f_3. In addition, we define the neutron detection efficiency of the BA1 as ε_{BA1} and the efficiency of the BA3 as ε_{BA3}. We measure $\varepsilon_{BA1} = 0.44$ and

$\varepsilon_{BA3} = 0.80$ in Table 8. We set the detection efficiency for a photon to be 100 % because the inefficiency is incorporated in the fraction f_2 itself. For example, the event with a photon not detected by the BA1 due to the inefficiency does not fall into the category (2), but into (1). The fraction of the events which have a hit in the BA1 is calculated to be $f_1 \times \varepsilon_{BA1} + f_2 \times 1.00$. The fraction of the events which have a hit in the BA3 is calculated to be $(f_1 + f_2) \times \varepsilon_{BA3}$ where a neutron only fires BA3. Out of 37 events, 26 events have hits in BA1, and 31 events have hits in BA3. The f_1, f_2 and f_3 are answers of the following equations:

$$
\begin{aligned}
31/37 &= (f_1 + f_2) \times \varepsilon_{BA3} && (1)\\
26/37 &= f_1 \times \varepsilon_{BA1} + f_2. && (2)\\
f3 &= 1 - (f_1 + f_2) && (3)
\end{aligned}
$$

By solving the equations, we get $f_1 = 0.62, f_2 = 0.43$, and $f_3 = -0.05$. The fraction f_3 is consistent with 0, which means that all 37 events have a neutron in the final state. We set $f_3 = 0$ which leads to $f_1 = 1 - f_2$. Then, we solve the equation again, which results in $f_2 = 0.47 \pm 0.13$ as shown in the paper [1].

Among 37 events, the events in the category (2) is vetoed anytime due to the photon hitting the BA1. Therefore, we only apply the neutron detection inefficiency to the events in the category (1). The number of background events is estimated to be $f_1 \times N_{events} \times (1 - \varepsilon_{BA}) = 37 \times (1 - 0.47) \times (1 - 0.82) = 3.5 \pm 0.9$ events.

The one event observed in the signal box is consistent with this expectation. In addition, in the P_T region above 260 MeV/c, we have 6 events without the BA requirements. The background level in this P_T range was estimated to be $f_1 \times N_{events} \times (1 - \varepsilon_{BA}) = 6 \times (1 - 0.47) \times (1 - 0.82) = 0.57 \pm 0.14$ events. This result is also consistent with one observed event.

7 Systematic Error

Uncertainties in the trigger efficiency, energy measurement, and the treatment of accidental activity in the MC are the main sources of the systematic error. The error on the acceptance ratio between $K_L \to \pi^0\nu\overline{\nu}$ and $K_L \to 2\pi^0$ is listed in Table 9 for each source since the error on the acceptance ratio could change the single event sensitivity of this search.

Source	$\Delta A(K_L \to \pi^0\nu\overline{\nu})/A(K_L \to 2\pi^0)$
Energy measurement	1 %
With and without accidental overlay	2.7 %
The ET board threshold	4.7 %
Total	5.5 %
$\delta BR(K_L \to 2\pi^0)/BR(K_L \to 3\pi^0)$	5.3 ± 3.7 %

Table 9: Sources of the systematic error. The $\delta BR(K_L \to 2\pi^0)/BR(K_L \to 3\pi^0)$ is the discrepancy between the measurement and the value in the PDG [5].

Each source of the error is explained as follows.

1. We add additional 1.5% energy smearing to the cluster energy in the MC. The energy smearing beyond 1.5% is unlikely, which disturbs the $K_L \to 2\pi^0$ mass distribution. By adding the energy smearing, we find 1% change on the acceptance ratio.

2. We calculate the acceptance ratio with and without accidental overlay in the MC. The difference of the acceptance ratio between with and without accidental overlay is found to be 2.7% in which the MC statistic has 2% error. Therefore, the change on the ratio is not found within the MC statistics. Even though, we assign the 2.7% change as the systematic error.

3. The threshold of the ET board is changed by $\pm$ 1 GeV from 4 GeV. The mean of the changes to both direction is 4.7%, which is assigned as the systematic error.

4. As a systematic check (not an error), we measured the well-known ratio of the branching ratios between $K_L \to 2\pi^0$ and $K_L \to 3\pi^0$. We measure $BR(K_L \to 3\pi^0)/BR(K_L \to 2\pi^0) = 214.2 \pm 5.9(\text{stat.})$, which is consistent with the PDG value 225.6 ± 5.6. The selection criteria for $K_L \to 3\pi^0$ is very similar as those for $K_L \to 2\pi^0$. The difference between this measurement and the PDG value is $5.3 \pm 3.7\%$, which is consistent with 0 within the current systematic uncertainty. This measurement supports the reliability of the normalization technique in which we use the decay with the different number of photons.

When we add all systematic errors in quadrature except for the value of $\delta BR(K_L \to 3\pi^0)/BR(K_L \to 2\pi^0)$, we get the 5.5% error as the total systematic error. At the end, we assign the 6 % systematic error in the acceptance ratio by raising decimals conservatively.

8 Final Result

Including the systematic error, the single event sensitivity for the decay $K_L \to \pi^0\nu\overline{\nu}$ in this experiment is:

$$\mathrm{SES}(\mathrm{K_L} \to \pi^0\nu\overline{\nu}) = [4.04 \pm 0.06(\mathrm{stat.}) \pm 0.24(\mathrm{sys.})] \times 10^{-7}.$$

As we expect the number of background events in Section 6, the remaining event is consistent with a background events from neutron interactions.

8.1 Treating the event as a signal

As a conservative way that we treat the last remaining event as a signal, the 90 % confidence upper limit on the number of $K_L \to \pi^0\nu\overline{\nu}$ event is:

$$\begin{aligned}
\mathrm{N}(\mathrm{K_L} \to \pi^0 \nu\overline{\nu})_{\mathrm{MAX\ in\ 90\%C.L.}} &= 3.89 * [1 + (3.89 - 1) * (0.06)^2/2] \\
&= 3.91 \text{ events},
\end{aligned}$$

where we use the equation (17c) in the reference [9].

The upper limit on the branching ratio is:

$$BR(K_L \to \pi^0 \nu\overline{\nu}) \ < \ 1.6 \times 10^{-6} \text{ (90\%C.L.)}.$$

8.2 Treating the event as a background

Since we believe that the last remaining event is background, we can get the 90 % confidence upper limit on the number of $K_L \to \pi^0 \nu\overline{\nu}$ event with the expected background events. The expected number of background events are 3.5 ± 0.9 events from neutron interactions including Λ decays, and 0.18 ± 0.18 events from kaon decays. Therefore, the total number of background estimation is 3.7 ± 0.9 events.

With the technique introduced in the PDG (page 166), the 90 % confidence upper limit on the number of $K_L \to \pi^0 \nu\overline{\nu}$ event is 2.77 event with the above background estimation. Including the systematic error with the equation (20) in the reference [9], the number goes to be 2.84 events. In this case, the upper limit on the branching ratio is:

$$BR(K_L \to \pi^0 \nu\overline{\nu}) \ < \ 1.2 \times 10^{-6} \text{ (90\%C.L.)}.$$

8.3 Conclusion

With a standard way, we take the conservative limit as the official result. The final result is:

$$BR(K_L \to \pi^0 \nu\overline{\nu}) \ < \ 1.6 \times 10^{-6} \text{ (90\%C.L.)}.$$

This result is by a factor of 36 improved than the best previous upper limit.

References

[1] The KTeV collaboration, "Search for the decay $K_L \to \pi^0 \nu\overline{\nu}$", will be submitted to PRL.

[2] See the KTeV log book on December 21st and 22nd in 1996.

[3] See the KTeV log book, page 299 on October 22nd in 1996.

[4] T. Nakaya, "Search for $K_L \to \pi^0 \nu\overline{\nu}$ with $\pi^0 \to \gamma\gamma$", presented at the E832 analysis(?) meeting in November, 1996.

[5] Particle Data Group, *Phys. Rev.* **D54**, S1 (1996).

[6] private communication with K. Hanagaki and S. Bright

[7] R. Coleman, KTeV library 0141.

[8] R. Kessler, KTeV library 0494.

[9] R. D. Cousins, *Nucl. Instrum. Methods* **A320**, 331 (1992).